Overview of the ETE Spherical Tokamak Experiment

E. Del Bosco, J.G. Ferreira, L.A. Berni, R.M. Oliveira, G.O. Ludwig,
C.S. Shibata, H. Patire Jr., J.O. Rossi, W.A. Vilela, L.F.W. Barbosa

Instituto Nacional de Pesquisas Espaciais – INPE
Laboratório Associado de Plasma – LAP
São José dos Campos – CEP 12.227-010 – SP– Brazil

This paper gives an overview of the ETE spherical tokamak activities in course at LAP/INPE, emphasizing the measurements of stray fields in the plasma region, produced mainly by eddy currents in the vacuum vessel, as well as measurements of gas breakdown and first plasma formation.

Introduction

The ETE spherical tokamak is a small size machine with some innovative technological features making possible a compact design with good access for plasma diagnosis. The main objectives of ETE are the investigation of operating regimes and confinement properties with emphasis on the plasma edge physics, as well as diagnostics development in fusion-related plasmas with low aspect ratio configuration.

The construction of ETE was initiated in 1995 and the first tokamak plasma was obtained by 28 November 2000. Presently, the experiments are focused on plasma formation, wall conditioning and diagnostics implementation. ETE was designed to reach inductive toroidal plasma current up to 400kA for about 100ms of time duration and confined by an external toroidal magnetic field of less than 0.8T. With the present low energy configuration of the capacitor banks (toroidal field – TF: 128kJ, ohmic heating – OH: 160kJ/single swing and equilibrium field – EF: 76kJ), plasma current of the order of 30kA was expected with duration up to 5ms. These values were practically achieved, with a maximum plasma current of 34kA lasting 2.6ms and a typical current of 21kA lasting 3.3ms.

Stray magnetic fields play an important role during the gas breakdown and plasma formation. Measurements of these fields without plasma are presented. It is shown that even with a relatively high eddy current in the vacuum vessel a null in the magnetic field configuration is formed, allowing the plasma formation. Plasma equilibrium is already achieved as confirmed by a CCD picture of the plasma cross-section. Optimization of the operating parameters, wall conditioning and increase of the capacitor banks energy is under way in order to reach the design values.

Apparatus

The assembly of the machine was completed successfully with an overall precision of about 2mm according to a very strict design. The central stack (ℓ = 1.87m, d = 168.8mm), which is composed by the 12 internal TF coil legs and by a two layers (130 turn each) solenoid was the most challenging piece completely manufactured in our laboratory. Table 1 gives the main parameters of the coils after assembling and the maximum currents actually obtained.

Baking of the vacuum vessel is presently limited to about 75^o C due to the lack of a thermal isolation blanket. During glow discharge cleaning a variable butterfly-like valve placed in front of the turbo-drag pump controls the gas flow. Viton O'rings are still fitted in a few ports. The minimum base pressure already achieved is about 10^{-7} mbar. A stainless steel frame (with electric insulation breaks) is placed inside the vessel in one toroidal location, holding bars of high purity graphite used as limiters. This frame also protects the Rogowski coil and a few magnetic pick-up coils. A total flux coil is also placed inside the vacuum vessel to measure the loop voltage at R = 0.443m.

Figure 1 presents the temporal current profiles of the three main coil circuits as well as the current induced in the vacuum vessel. The coil currents shown are the maximum obtained in the present configuration of the capacitor banks. The current rise in the TF coil is obtained by firing a fast bank (0.9kV) and the flat top (10ms) is maintained by firing three slow banks (90V each). The toroidal field at R = 0.3m is about 0.0078T/kA. The current waveform in the equilibrium coil is pre-programmed using one fast bank (2kV) and two slow banks (200V each). The maximum vertical field is about 35mT obtained when eddy currents in the vessel have already decayed. The current rise in the OH coil is produced by discharging a fast bank (4kV), which breaks down the gas insulation, and the plasma current is maintained by firing one slow bank (2kV). The maximum induced voltage at R_0 due to the OH coil is about 7.2V. This value can reach about 10V when the equilibrium field is also present.

Coil	R (mm)	Z (mm)	Turns	I (kA)
Solenoid	72.7	0	2×130	~ 4
Compensation 1	102	± 657	2×10	~ 4
Compensation 2	651	± 883	1×2	~ 4
Elongation	200	± 830	4×4	-
Equilibrium	700	± 422	4×4	~ 2
Toroidal	-	-	12 D-shaped in series	~ 11

Table 1. Parameters of the coils

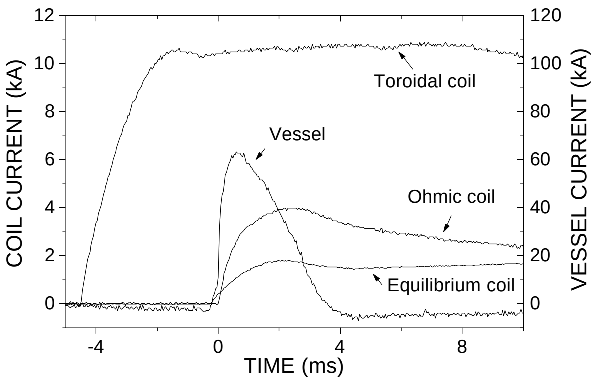

Figure 1. Waveforms of the currents in the coils and current induced in the vacuum vessel

Stray fields

Stray fields in the plasma region can be generated by several means: bad compensation of the solenoid, misalignment of poloidal coils, bending of TF coils, and induced currents. These fields are undesirable during plasma formation since they can prevent gas breakdown. Because the vacuum vessel of ETE has no electrical break in the toroidal direction relatively high values are expected for the current induced on its walls, notwithstanding the high electrical resistive Inconel alloy used in its manufacture. This current is in opposite direction relative to the currents in the coils, reaching its peak at the very beginning of the poloidal field bank discharges. Preliminary measurements of these stray fields were carried out and are presented in the following.

Figure 2 shows the radial profiles of the vertical magnetic field (B_z) due to the equilibrium (open squares), ohmic heating (open circles) and toroidal (open triangles) circuits as well as the total B_z produced by firing all banks together (solid squares and line). The fields were measured approximately at 0.2ms after triggering the OH bank, which corresponds roughly to the instant of breakdown. The values of the coil and vessel currents in that instant of time are also shown in the picture. It can be observed from figure 2 that the total B_z profile crosses the zero-axis at R ~ 0.45m. It is noteworthy to point out that the vertical equilibrium field (open squares) is not a stray field; on the contrary, its trigger time is experimentally adjusted in order to compensate for the stray fields creating the null point. Figure 3 shows the radial profile of the radial magnetic field, B_r, generated by the ohmic heating (solid circles) and equilibrium (open squares) circuits for the same conditions of figure 2.

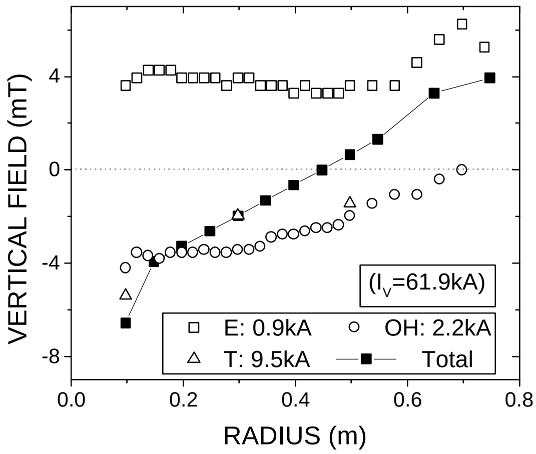

Figure 2. B_z radial profile due to ohmic heating, equilibrium and toroidal coil currents

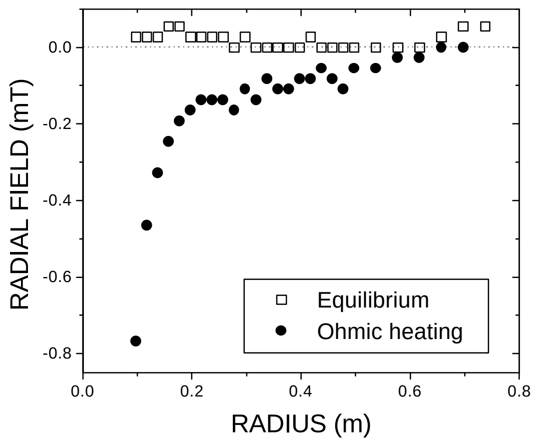

Figure 3. B_r radial profile due to ohmic heating and equilibrium coil currents

Figure 4 shows the radial profile of the vertical magnetic field, B_z, (solid squares) created by the OH coils alone when the value of the coil current reaches its maximum (3.9 kA). At this instant the induced current in the vessel is 19.5kA in the opposite direction. The dash-dotted line represents the calculated profile taking into account only the OH coils, while the dashed line is the profile computed modeling the vessel as 32 filaments. The solid line is the total calculated profile. The filaments and currents distribution in the vessel are being optimized considering measurements of the current taken in different parts of the vessel with the ports open, as well as the thickness of the wall around the poloidal plane. Figure 5 shows the B_z radial profile for the equilibrium coils at two different instants of the same shot: the open squares represent the instant when the induced current in the vessel is high (20.9kA) while the solid squares are taken when the induced current has already decayed to zero. In both profiles the current in the coils is about the same, 1.8kA. The lines in figure 5 are calculated profiles; the dashed one is for I_{vessel} = 20.9kA while the solid one is for I_{vessel} = 0.

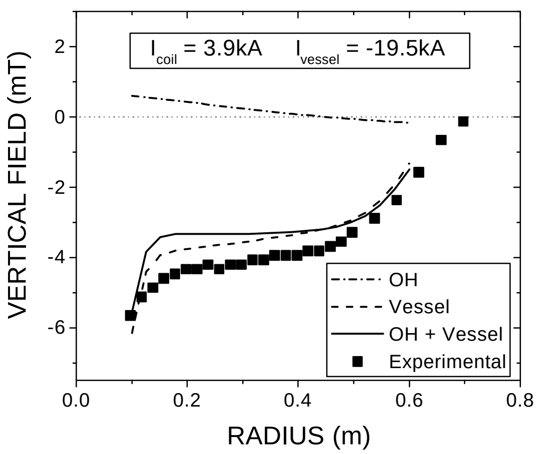

Figure 4. B_z radial profile due to the ohmic heating coil current and calculated profiles

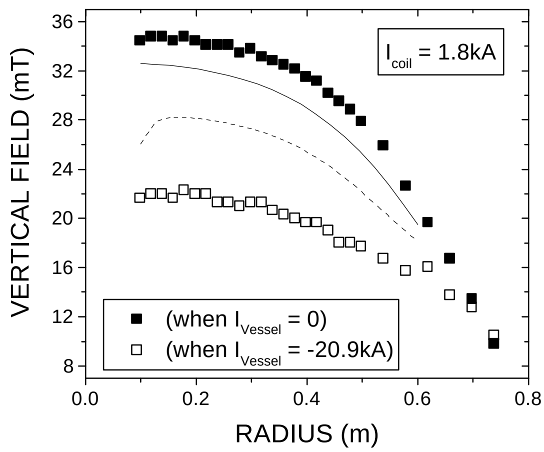

Figure 5. B_z radial profile due to the equilibrium coil current and calculated profiles

Breakdown

A preliminary study of the gas breakdown in ETE was carried out. The characteristic breakdown curve, electric field versus gas pressure, and the time lag versus gas pressure were measured for three different conditions: no pre-ionization, UV lamp, and hot filament pre-ionization (4A×47V, 75V polarization). Figure 6 shows the E×P curves and figure 7 shows the $\tau_{lag}\times P$ curves. The electric field was measured with a total flux coil placed inside the vessel. The time lag was defined as the time interval between the application of the OH bank and the beginning of the plasma current. Hydrogen gas was continuously supplied and the pressure was measured with an ion gauge. The beneficial effect of pre-ionization is clearly observed in these figures. Electric field values as low as 2V/m are enough for breakdown.

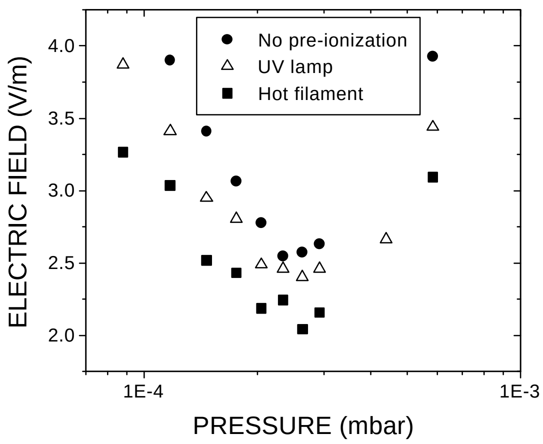

Figure 6. E×P curves for H_2 breakdown in ETE.

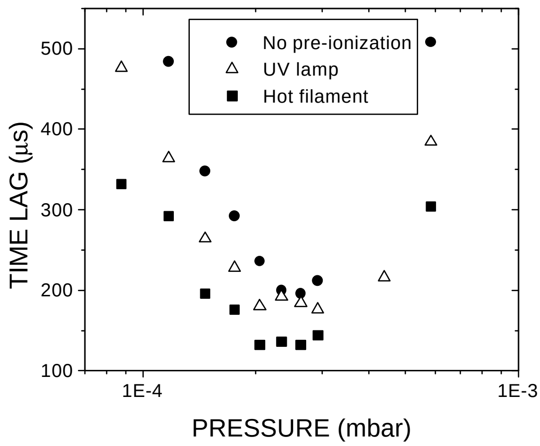

Figure 7. Time lag for gas breakdown in ETE

Equilibrium

The equilibrium of the plasma current in ETE was confirmed using a high-speed CCD camera. Figure 8 shows the picture of the plasma cross-section taken during shot 1404, when the plasma current was about 8kA. The D-shaped cross section of the plasma is clearly observed.

Figure 8. CCD photo of the plasma cross section

Conclusions

The ETE spherical tokamak was successfully assembled. The first plasma was obtained by the end of 2000. The eddy current in the vacuum vessel is being modeled in order to optimize the gas breakdown and plasma formation. By properly setting the time delay between the ohmic heating and vertical banks, the gas breakdown is easily obtained even without pre-ionization. Plasma equilibrium is being achieved. Wall conditioning (DC glow and baking) is now under way in order to increase the plasma current as well as the discharge duration. Capacitor banks have to be completed in order to reach the design values.

Acknowledgments: The authors give thanks to FAPESP, Finep, CNPq and IAEA for financial support and Dr. O. Mendes (CEA/INPE) for loaning the fast CCD camera.